THE JOURNAL OF PHYSICAL CHEMISTRY Letters

Letter

pubs.acs.org/JPCL

A Look at the Origin and Magnitude of the Chemical Contribution to the Enhancement Mechanism of Surface-Enhanced Raman Spectroscopy (SERS): Theory and Experiment

Nicholas Valley,‡ Nathan Greeneltch,‡ Richard P. Van Duyne, and George C. Schatz*

Department of Chemistry, Northwestern University, Evanston, Illinois 60208-3113, United States

Supporting Information

ABSTRACT: Normal and surface-enhanced Raman spectra for a set of substituted benzenethiols were measured experimentally and calculated from static polarizability derivatives determined with time-dependent density functional theory (TDDFT). Both silver and gold cluster−thiolate complexes were studied to investigate how the chemical enhancement varies with substituent. The experimental relative peak intensities and positions are well-matched by their theoretical counterparts. The static chemical enhancement of the ring stretching modes near 1600 cm^{-1} is determined experimentally and computationally for each derivative, and it is found that the experimental enhancement varies by a factor of 10 as a result of chemical substitution, with stronger electron donating groups on the benzene unit leading to higher enhancements. The calculated trends with substitution match experiment well, suggesting that TDDFT is describing the chemical effect qualitatively, if not quantitatively, in the static (low-frequency) limit. A two-state model is developed, providing qualitative insight into the results in terms of the variation of ligand-to-metal charge-transfer excitation energy with substitution.

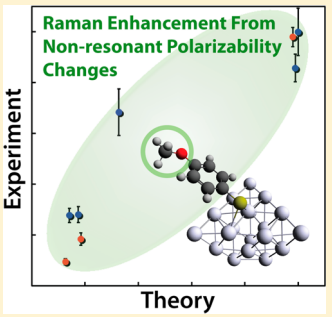

SECTION: Spectroscopy, Photochemistry, and Excited States

Raman spectroscopy induces and interrogates inelastic scattering of light by molecules, with the scattered light providing a vibrational fingerprint unique to each molecule. This inherently weak process has been shown to be greatly enhanced when molecules are adsorbed onto noble-metal surfaces.[1] This leads to surface-enhanced Raman scattering (SERS), a powerful analytical tool. Signal enhancement is widely attributed in literature[2−5] to two main mechanisms: the chemical enhancement (CE) and electromagnetic (EM) mechanisms.

The EM[6,7] involves amplification of the local electric field at the molecule's position due to plasmon excitation of the metallic structure. Enhancements in the range of 10^4 to 10^8 are commonly reported. There is good evidence that this mechanism governs the dependence of the SERS signal on nanoparticle morphology. The CE mechanism is not as well understood, but it is postulated to arise from three distinct processes:[8−10] enhancements from molecular excitation resonances, charge-transfer resonances, and nonresonant changes in the molecular polarizability that occur upon adsorption onto the metal surface. There have been attempts to develop theories that include all contributions of the SERS effect together, such as work by Lombardi et al. based on Herzberg−Teller relations.[9,11] However, investigating these effects separately allows for the magnitude of each contribution to be isolated and quantified.

Herein we focus on the third CE mechanism, which is also called the static chemical enhancement (CHEM). This enhancement mechanism is intrinsically linked with the creation of a new chemical system (i.e., the metal−molecule complex) leading to changes in the polarizability and vibrational modes of the molecular moeity. Changes in the molecular polarizability upon binding are believed to lead to enhancements in the range of $\sim 10^0$ to 10^3 for Raman scattering,[5,12,13] but this estimate carries uncertainty due to the lack of careful theory/experiment comparisons. Recently, Morton and Jensen have proposed a two-state model for studying the static CHEM enhancement.[14] They used TDDFT calculations in the static (low-frequency) limit for molecules adsorbed onto silver clusters to define the chemical enhancement factor (through comparison with the calculated intensity in the absence of surfaces). They found that molecule−metal systems that stabilize pi backbonding provide an enhancement to the attached molecule's polarizability and hence to enhanced Raman scattering. They argued that calculations of this effect for small silver clusters would give results similar to realistic SERS nanoparticle substrates, as the static limit Raman intensity is only weakly dependent on cluster size. The chemical enhancement factor they calculated was purely theoretical; however, comparisons of the TDDFT results with a two-state model were provided to reveal the analytical origin of the effect. This comparison showed that the enhancement factor typically depends on the energy gap between the HOMO of the cluster and the LUMO of the adsorbed molecule, as is physically plausible. However a concern with this formulation is

Received: June 14, 2013
Accepted: July 22, 2013

 © XXXX American Chemical Society dx.doi.org/10.1021/jz4012383 | J. Phys. Chem. Lett. 2013, 4, 2599−2604

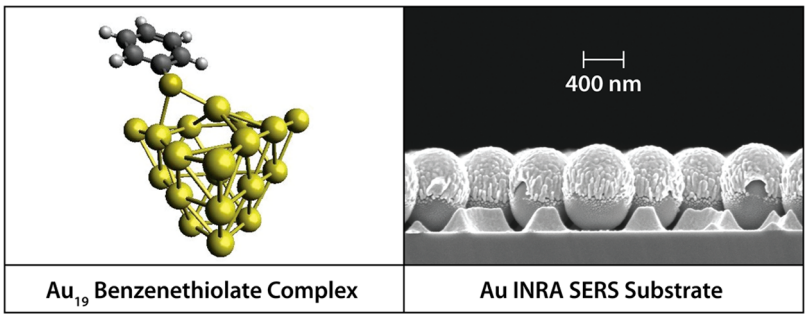

Figure 1. Left pane: Structure of the Au_{19}–benzenethiolate complex used in TDDFT calculations. The metal cluster is constructed by truncating one vertex of a 20 atom tetrahedral cluster. Right pane: Surface of gold INRA SERS substrate used for Raman experiments. The substrates were fabricated by depositing 200 nm of metal over 600 nm silica microspheres.

Table 1. Vibrational Mode Energies for Benzenethiol and Benzenethiol–Metal Complexes[a]

BT (cm^{-1})	Ag-BT (cm^{-1})	Au-BT (cm^{-1})	exp. BT (cm^{-1})	exp. Ag-BT (cm^{-1})	exp. Au-BT (cm^{-1})	mode description
689.6	682.9	683.4	699	688	688	ring and C–S stretch
989.3	987.6	988.3	1000	996	996	ring breathing
1017.5	1013.1	1013.3	1025	1018	1018	ring breathing
1073.6 1079.9	1054.3	1054.1	1092	1068	1069	ring breathing and C–S stretch
1578.0	1564.7	1565.1	1584	1573	1573	C–C stretch

[a]First three columns on the left are from TDDFT calculations, while columns denoted "exp" represent modes observed experimentally. Experimental SERS spectra were recorded using metal INRA SERS substrates.

that pure density functionals tend to underestimate energy gaps between occupied and virtual states, so it was not clear that the chemical effects were correctly described. We show, with extensive comparisons to experiment, that the same level of theory (TDDFT in the static limit) can reliably calculate the contribution of adsorption-induced nonresonant molecular polarizability changes to the SERS effect.

Substrates used in SERS studies usually consist of Ag or Au nanoparticles[7,15] or roughened surfaces.[16−18] In general, such substrates are designed to provide large EM enhancement, albeit with considerable spot-to-spot signal variation across the surface. For this work, it is important to have uniform EM enhancement over large areas,[19,20] as this simplifies the separation of EM and CE. Both silver and gold immobilized nanorod assembly (INRA)[21,22] substrates have been shown to possess these traits, leading to their use in this work.

Theoretical static SERS spectra including chemical effects have been generated by incorporating a small metal cluster into the TDDFT calculations. This follows our previous work, where a 20 atom cluster with approximately tetrahedral shape was found to provide a reasonable model of a (111) surface (any of the faces of the tetrahedron) upon which a molecule is adsorbed.[12,13] In the present application, this choice is complicated by the thiol molecule's propensity to undergo chemisorption on these surfaces. After studying several alternatives, we chose a Ag_{19}/Au_{19}–thiolate complex, with the vertex atom opposite the adsorption site removed, as this closed-shell structure provides spectra with the best experimental agreement. A representative structure of modeled molecule–metal complexes is shown in Figure 1. Geometry optimizations were performed utilizing a starting structure with the sulfur above the central metal atom on the triangular cluster face. Local minima correspond to structures where sulfur bridges two metal atoms. For the gold clusters, some of the benzenethiol derivatives also have a local minimum structure with sulfur bound to the central metal atom of the face. However, these structures were always higher in energy than the bridging structures. The bridging structures were therefore chosen as the metal–molecule complex used to calculate SERS spectra. Note: this bridging structure is related to S–Au–S bridges thought to be important for arylthiolates adsorbed onto small gold clusters[23−26] and on Au(111) surfaces.[27]

Seven molecules were studied experimentally and theoretically using both gold and silver substrates. Not all molecules were stable on the metal substrates, leading to a smaller experimental data set with eight molecule/surface combinations. Chemical enhancement factors (EFs) were determined for three molecules on silver surfaces: benzenethiol (BT), 4-mercaptophenol (MP), and 4-mercaptobenzoic acid (MBA) and five on gold surfaces: BT, MBA, 4-methoxybenzenethiol (MBT), 4-ethoxybezenethiol (EBT), and 4-nitrobenzenethiol (NBT).

Calculated energies of the benzenethiol derivatives' vibrational modes are shifted when the molecules are bound to the clusters. Select normal mode energies are presented in Table 1 for benzenethiol in the gas phase and bound to silver and gold clusters. Large shifts occur for the ring-breathing mode near 1060 cm^{-1} and the ring C–C stretches near 1570 cm^{-1}, while the modes at ∼612 and 988 cm^{-1} see minor changes. Cartesian coordinates and vibrational normal modes between 300 and 2000 cm^{-1} for all optimized structures and detailed comparisons of calculated and experimental spectra can be found in the Supporting Information. To further verify our theoretical description of normal and SERS spectra as well as the static chemical effects involved, CHEM EFs for several vibrational modes of each molecule were determined. A linear trend is expected when comparing theoretical and experimental results if the theoretical model is a reasonable representation of the experimental system. This technique has been previously used by Zayak et al. to determine surface binding geometries.[28] This analysis is also independent of the surface coverage of the molecules (as long as there is no change in binding geometry).

dx.doi.org/10.1021/jz4012383 | J. Phys. Chem. Lett. 2013, 4, 2599−2604

Peaks were chosen for analysis if they were present in both the normal and SERS experimental spectra. As expected, some peaks in the solution Raman spectra were obscured by solvent.

Vibrational modes that could be properly analyzed are plotted in Figure 2. For clarity, EFs for each peak are scaled

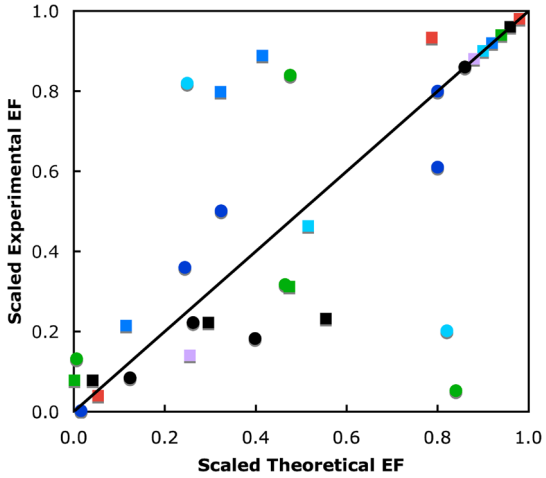

Figure 2. Comparison of scaled experimental and simulated enhancement factors for various modes of the molecule and choice of substrate. Circles denote Ag substrate, squares denote Au substrate. Colors denote the substituted benzenethiol: BT (black), NBT (red), MBT (green), EBT (light blue), MP (blue), MA (purple). The straight line is $y = x$. Experimental SERS spectra were recorded using metal INRA SERS substrates.

such that the largest EF for each molecule is set in the range 0.8 to 1.0. Values for NBT and MA on silver are not included because these molecules undergo an induced photoreaction.[29,30] Only a single peak (~1600 cm^{-1}) was sufficiently differentiated from solvent for MBA on both metals. Of the remaining combinations, the MP on gold and the MBT and EBT on silver show very poor agreement of calculated and experimental chemical EFs. For these complexes, it is possible that molecules were bound to the surface in a geometry different from what was assumed. Also, extensive delamination was observed for EBT on the silver INRA substrates. It is likely that the MP and MBT are delaminating similarly on a smaller scale. Because this behavior results in unreliable EFs, these combinations were not considered in further analysis. Comparisons involving the remaining molecules result in linear behavior, with slopes near unity and intercepts near zero. The EF calculation[31] used for this study is described in detail in the Supporting Information.

Chemical EFs for the set of peaks occurring at ~1600 cm^{-1} for each of the benzenethiol derivatives determined from experiment and TDDFT calculations are shown in Table 2. Peaks at ~1600 cm^{-1} were chosen because they are clear of interference (including solvent peaks) in the experimental SERS and normal Raman spectra for the entire molecule set. The spectra corresponding to the silver SERS measurements are included in Figure 3. Vibrational modes of the two peaks near 1600 cm^{-1} included in the EF calculations are the two nearly degenerate ring-stretching modes shown in Figure 4. The position and splitting of these modes are dependent on the identity of the substituent. Whether one or two peaks were observed experimentally in this spectral region, the entire area under the curve was used to calculate EFs.

Table 2. Chemical Enhancement Factors Determined from Experiments and Calculated Using TDDFT[a]

	experimental 1600 cm^{-1} EF (scaled)	TDDFT 1600 cm^{-1} EF (absolute)
Au–		
$-OC_2H_5$	53.1	111.0
$-OCH_3$	45.5	109.8
–H	36.3	36.3
$-CO_2H$	14.7	15.7
$-NO_2$	14.9	19.4
Ag–		
–OH	60.5	60.6
–H	11.4	11.4
$-CO_2H$	5.9	7.8

[a]Experimental EF values for each metal were scaled relative to the benzenethiol result, with BT being scaled equal to the corresponding theoretical value. Experimental SERS spectra were recorded using metal INRA SERS substrates.

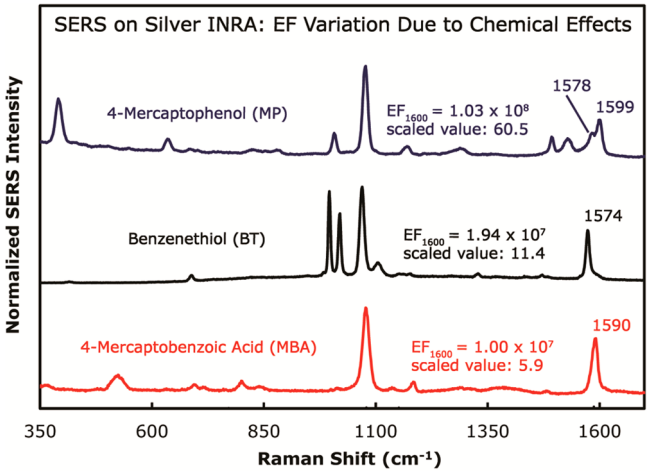

Figure 3. SERS spectra of benzenethiol derivatives on AgINRA surface. All measurements were made with a 785 nm excitation source. The EF_{1600} values reported correspond to the enhancements calculated using the singlet or doublet of peaks found ~1600 cm^{-1}.

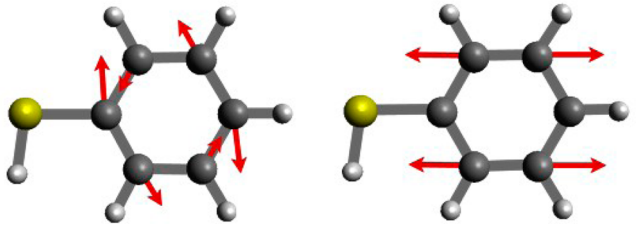

Figure 4. Vibrational motions of benzenethiol near 1600 cm^{-1} chosen for EF comparison in Table 2 and Figure 5.

Effects due to molecular resonances were avoided by using incident light (785 nm) not energetic enough to electronically excite any states associated with the molecules considered.[32] The enhancement observed is therefore a combination of the EM enhancement from the plasmonic substrate and a static chemical effect due to ground-state molecule–surface interactions. Dividing the SERS intensity per molecule by the normal Raman intensity per molecule gives an EF measurement that is composed only of the EM enhancement (from the substrate) and of static chemical effects. The uniformity[21] of the INRA substrate assures that the EM enhancement is a constant

dx.doi.org/10.1021/jz4012383 | J. Phys. Chem. Lett. 2013, 4, 2599–2604

contributor. Thus the variation in measured EF for different molecules is a direct reflection of the static chemical enhancement. Theoretical calculations of the Raman spectra were performed in the static limit to determine Raman cross sections for both the free thiol and the corresponding thiolate−metal cluster complex.

Figure 5 presents the comparison of experimental and simulated EFs for the 1600 cm^{-1} peaks. In contrast with Figure 2, this plot shows a more linear relationship between experiment and theory, with both data showing an increase in enhancement as the substituent group becomes more electron-donating. Linear fitting of the data gives a slope near unity, suggesting that TDDFT is reasonably accurate in calculation of relative chemical EFs.

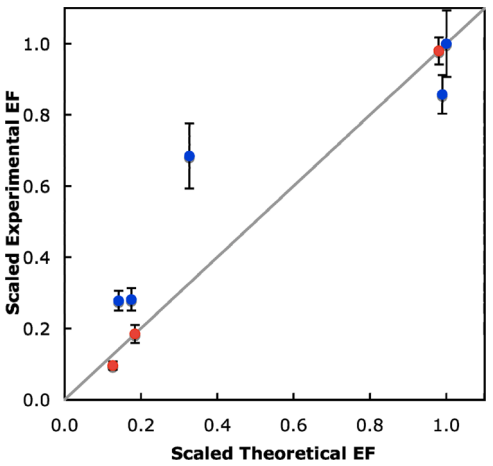

Figure 5. Comparison of scaled experimental and simulated enhancement factors for the 1600 cm^{-1} peak(s). Ag complexes are red points. Au complexes are blue points. The gray line is $y = x$. Experimental SERS spectra were recorded using metal INRA SERS substrates.

The absolute CHEM EFs are calculated to be between 10^1 and 10^2, which is in the range expected based on previous work.[14] On gold, the relative enhancements from highest to lowest vary by a factor of 3.6 in the experimental measurements and a factor of 7 in the density functional calculations. On silver, the factors are 10.3 and 8, respectively. In agreement with other studies,[33] the absolute CHEM enhancements were calculated to be larger on gold than on silver. This is due to the lower energy of the LUMO of the gold cluster than that of the silver cluster, as previously noted by Morton et al.[8] Both theory and experiment agree that the electron-donating substituents give rise to the largest CHEM enhancement.

Now let us consider comparisons of the experimental and theory results with those from the two-state model developed by Morton and Jensen. Table 3 displays the comparison of experimental and TDDFT integrated EFs with two-state model results. Assuming as was done in previous studies of pyridine derivatives that the important transition is the metal HOMO to molecule LUMO (metal-to-ligand charge transfer or "MLCT"), the two-state model predicts a reduction in intensity that is unphysical in nature. Considering instead a molecular HOMO to metal LUMO transition[8] (ligand-to-metal charge transfer or "LMCT"), the experimental, TDDFT, and two-state model results all display the same trend. Note: Exact agreement is not expected with the approximations made in this simple model. In addition, there are uncertainties in how the experimental and TDDFT EFs are determined depending on which vibrational modes are chosen for comparison.

For the experimental EFs only, the observed peaks for each molecule rather than all vibrational modes were selected for comparison. In the TDDFT results, we can either choose the same modes as in the experiment or we can integrate over all modes. To see the size of the difference between the results, TDDFT-integrated EFs were calculated using both the full range of peaks between 500 and 2000 cm^{-1} and the subset (labeled "partial" in Table 3) used for the experimental determination. The results show variations by a factor of 2 for some substituents. The comparisons between experiment and TDDFT are generally improved by the partial selection procedure. The two-state model shows trends with substituents that are greatly exaggerated compared with either experiment or TDDFT but are qualitatively similar. We must emphasize that the two-state model is a simplification and in the present application we have used a and b factors from the study by Morton and Jensen, which assumed a MLCT mechanism. It is not clear from our work if revising these parameters for the LMCT version of the model would improve comparisons with TDDFT.

To summarize, it was shown through comparison with experiment that TDDFT with a BT-Ag_{19} or BT-Au_{19} "SERS" model accurately predicts chemical EFs across a range of substituted benzenethiols. The calculations provided a satisfactory prediction of relative chemical enhancements for peaks within the same spectrum. These calculations show that there is a modest CHEM enhancement in the range of $\sim 10^0$ to

Table 3. Integrated Enhancement Factors Determined from Experiments, Calculated Using TDDFT, and Calculated Using a Two-State Model Considering Two Different Sets of States[a]

	experimental integrated EF ($\times 10^6$)	TDDFT integrated EF	TDDFT partial integrated EF	MLCT two-state EF	LMCT two-state EF
Au−					
$-OC_2H_5$	66	51	140	0.03	780
$-OCH_3$	38	54	66	0.03	900
−H	31	24	28	0.12	88
$-CO_2H$	10	15	16	0.13	7.4
$-NO_2$	23	13	25	0.18	1.3
Ag−					
−OH	58	27	46	0.02	24
−H	20	10	12	0.04	29
$-CO_2H$	19	8.0	7.8	0.54	0.25

[a]Experimental SERS spectra were recorded using metal INRA SERS substrates.

dx.doi.org/10.1021/jz4012383 | J. Phys. Chem. Lett. 2013, 4, 2599−2604

10^2 for substituted benzenethiols, with more strongly donating groups leading to larger enhancements. The two-state model proved to be useful for "rough" comparison between theory and experiment; however, we found that it was necessary to use the LMCT energy gap to determine meaningful EFs from this model, while using the MLCT gap results even in qualitative errors.

EXPERIMENTAL METHODS

BT, MP, MBT, NBT, and MBA were used as received from Sigma-Aldrich. EBT was purchased from Santa Cruz Biotechnology. All solvents were purchased from Sigma-Aldrich. BT, MP, MBT, and EBT were used for overnight incubation at 150 mM in ethanol. NBT and MBA were prepared at the same concentration in acetone and isopropanol, respectively.

Metal INRA SERS substrates were fabricated as previously described.[21,22] Gold and silver films (200 nm thick) were deposited at a rate of 1 Å·s^{-1} under high vacuum (2.0×10^{-7} Torr) over the nanosphere-covered surface using thermal vapor deposition (Kurt J. Lesker, PVD 75). The metal mass thickness and deposition rate were measured by a 6 MHz gold-plated quartz crystal microbalance (Sigma Instruments, SQM-160). The gold INRA surfaces were plasma-cleaned for 5 min with 99.999% O_2 in a refractive ion etcher (South Bay Technology, RIE-2000) at 196 mT and 51 W. An inverted microscope (Nikon Eclipse Ti) was used for all Raman measurements. An Innovative Photonics Solutions stabilized 785 nm diode laser was used for single-frequency experiments. The detection system was an imaging spectrograph (Acton SpectraPro 2300i) with an LN_2-cooled back-thinned deep-depletion CCD detector (Roper, model spec 10:400 BR, 1340 × 400 pixels). The source was directed through the back entrance of the microscope and focused down to a 70 μm × 70 μm spot onto the opaque metal INRA substrates using a 20× microscope objective (wd = 2.1 mm).

Computational Methods. Calculations presented in this work were performed using the Amsterdam Density Functional (ADF) program package.[34] Full geometry optimization and frequency calculations for isolated benzenethiols and the molecule−metal cluster complexes were completed. A gradient-corrected Becke−Perdew (BP86) exchange−correlation functional was used with a triple-ζ polarized Slater-type (TZP) basis set for all atoms. Polarizabilities were calculated using the AOResponse module with the same level of theory. Scalar relativistic effects were accounted for with the zeroth order regular approximation (ZORA). Raman intensities were calculated from static polarizabilities, as outlined in the Supporting Information.

ASSOCIATED CONTENT

Supporting Information

Optimized geometries, vibrational frequencies, and theoretical and experimental Raman spectra of all molecules. Example experimental Raman and SERS measurements along with an EF calculation and further theory computational detail. This material is available free of charge via the Internet at http://pubs.acs.org.

AUTHOR INFORMATION

Corresponding Author

*E-mail: schatz@chem.northwestern.edu.

Author Contributions

‡Nicholas Valley and Nathan Greeneltch contributed equally. The manuscript was written through contributions of all authors. All authors have given approval to the final version of the manuscript.

Notes

The authors declare no competing financial interest.

ACKNOWLEDGMENTS

This work was supported by the National Science Foundation (CHE-0911145, CHE-1152547, DMR-1121262), the Defense Advanced Research Projects Agency (N66001-11-1-4179 and FA9550-08-1-0221), and the Department of Energy's Office of Basic Energy Science (SISGR DE-FG02-09ER16109). The SEM image in Figure 1 was recorded by Dr. Anne-Isabelle Henry at Northwestern University's Electron Probe Instrumentation Center (EPIC) and is used with permission.

REFERENCES

(1) Jeanmaire, D. L.; Van, D. R. P. Surface Raman Spectroelectrochemistry. Part I. Heterocyclic, Aromatic, and Aliphatic Amines Adsorbed on the Anodized Silver Electrode. *J. Electroanal. Chem. Interfacial Electrochem* **1977**, *84*, 1−20.

(2) Tong, L. M.; Zhu, T.; Liu, Z. F. Approaching the Electromagnetic Mechanism of Surface-Enhanced Raman Scattering: From Self-Assembled Arrays to Individual Gold Nanoparticles. *Chem. Soc. Rev.* **2011**, *40*, 1296−1304.

(3) Qian, X. M.; Nie, S. M. Single-Molecule and Single-Nanoparticle SERS: From Fundamental Mechanisms to Biomedical Applications. *Chem. Soc. Rev.* **2008**, *37*, 912−20.

(4) Campion, A.; Kambhampati, P. Surface-Enhanced Raman Scattering. *Chem. Soc. Rev.* **1998**, *27*, 241−250.

(5) Morton, S. M.; Silverstein, D. W.; Jensen, L. Theoretical Studies of Plasmonics Using Electronic Structure Methods. *Chem. Rev.* **2011**, *111*, 3962−94.

(6) Schatz, G. C.; Young, M. A.; Van Duyne, R. P. Electromagnetic Mechanism of SERS. In *Surface-Enhanced Raman Scattering: Physics and Applications*; Springer-Verlag: Berlin, 2006; Vol. *103*, pp 19−45.

(7) Gersten, J.; Nitzan, A. Electromagnetic Theory of Enhanced Raman Scattering by Molecules Adsorbed on Rough Surfaces. *J. Chem. Phys.* **1980**, *73*, 3023−3037.

(8) Morton, S. M.; Ewusi-Annan, E.; Jensen, L. Controlling the Non-Resonant Chemical Mechanism of Sers Using a Molecular Photoswitch. *Phys. Chem. Chem. Phys.* **2009**, *11*, 7424−7429.

(9) Lombardi, J. R.; Birke, R. L. A Unified Approach to Surface-Enhanced Raman Spectroscopy. *J. Phys. Chem. C* **2008**, *112*, 5605−5617.

(10) Kambhampati, P.; Child, C. M.; Foster, M. C.; Campion, A. On the Chemical Mechanism of Surface Enhanced Raman Scattering: Experiment and Theory. *J. Chem. Phys.* **1998**, *108*, 5013−5026.

(11) Lombardi, J. R.; Birke, R. L.; Lu, T. H.; Xu, J. Charge-Transfer Theory of Surface Enhanced Raman Spectroscopy: Herzberg-Teller Contributions. *J. Chem. Phys.* **1986**, *84*, 4174−4180.

(12) Zhao, L. L.; Jensen, L.; Schatz, G. C. Pyridine-Ag-20 Cluster: A Model System for Studying Surface-Enhanced Raman Scattering. *J. Am. Chem. Soc.* **2006**, *128*, 2911−2919.

(13) Jensen, L.; Zhao, L. L.; Schatz, G. C. Size-Dependence of the Enhanced Raman Scattering of Pyridine Adsorbed on Ag-N (N=2−8, 20) Clusters. *J. Phys. Chem. C* **2007**, *111*, 4756−4764.

(14) Morton, S. M.; Jensen, L. Understanding the Molecule-Surface Chemical Coupling in SERS. *J. Am. Chem. Soc.* **2009**, *131*, 4090−4098.

(15) Lee, P. C.; Meisel, D. Adsorption and Surface-Enhanced Raman of Dyes on Silver and Gold Sols. *J. Phys. Chem.* **1982**, *86*, 3391−3395.

(16) Fleischmann, M.; Hendra, P. J.; McQuillan, A. J. Raman Spectra of Pyridine Adsorbed at a Silver Electrode. *Chem. Phys. Lett.* **1974**, *26*, 163−166.

(17) Jin, M.; van Wolferen, H.; Wormeester, H.; van den Berg, A.; Carlen, E. T. Large-Area Nanogap Plasmon Resonator Arrays for Plasmonics Applications. *Nanoscale* **2012**, *4*, 4712−4718.
(18) Qiuming, Y.; Scott, B.; Brian, C.; Jiajie, X.; Paul, M. W.; Heng, G.; Dmitry, K. Surface-Enhanced Raman Scattering on Gold Quasi-3d Nanostructure and 2d Nanohole Arrays. *Nanotechnology* **2010**, *21*, 355301.
(19) Park, S. G.; Hwang, H.; Yang, S. M. Fabrication of Highly Uniform Three-Dimensional Sers Substrates by Control of Wettability. *J. Mater. Chem. C* **2013**, *1*, 426−431.
(20) Pazos-Perez, N.; Ni, W. H.; Schweikart, A.; Alvarez-Puebla, R. A.; Fery, A.; Liz-Marzan, L. M. Highly Uniform Sers Substrates Formed by Wrinkle-Confined Drying of Gold Colloids. *Chem. Sci.* **2010**, *1*, 174−178.
(21) Greeneltch, N. G.; Blaber, M. G.; Henry, A.-I.; Schatz, G. C.; Van Duyne, R. P. Immobilized Nanorod Assemblies: Fabrication and Understanding of Large Area Surface-Enhanced Raman Spectroscopy Substrates. *Anal. Chem.* **2013**, *85*, 2297−2303.
(22) Greeneltch, N. G.; Blaber, M. G.; Schatz, G. C.; Van Duyne, R. P. Plasmon-Sampled Surface-Enhanced Raman Excitation Spectroscopy on Silver Immobilized Nanorod Assemblies and Optimization for near Infrared (Λex = 1064 nm) Studies. *J. Phys. Chem. C* **2012**, *117*, 2554−2558.
(23) Akola, J.; Walter, M.; Whetten, R. L.; Hakkinen, H.; Gronbeck, H. On the Structure of Thiolate-Protected Au-25. *J. Am. Chem. Soc.* **2008**, *130*, 3756−3757.
(24) Heaven, M. W.; Dass, A.; White, P. S.; Holt, K. M.; Murray, R. W. Crystal Structure of the Gold Nanoparticle [N(C8h17)(4)][Au-25(Sch2ch2ph)(18)]. *J. Am. Chem. Soc.* **2008**, *130*, 3754−3755.
(25) Zhu, M.; Aikens, C. M.; Hollander, F. J.; Schatz, G. C.; Jin, R. Correlating the Crystal Structure of a Thiol-Protected Au-25 Cluster and Optical Properties. *J. Am. Chem. Soc.* **2008**, *130*, 5883−5885.
(26) Jadzinsky, P. D.; Calero, G.; Ackerson, C. J.; Bushnell, D. A.; Kornberg, R. D. Structure of a Thiol Monolayer-Protected Gold Nanoparticle at 1.1 Angstrom Resolution. *Science* **2007**, *318*, 430−433.
(27) Cossaro, A.; Mazzarello, R.; Rousseau, R.; Casalis, L.; Verdini, A.; Kohlmeyer, A.; Floreano, L.; Scandolo, S.; Morgante, A.; Klein, M. L.; Scoles, G. X-Ray Diffraction and Computation Yield the Structure of Alkanethiols on Gold(111). *Science* **2008**, *321*, 943−946.
(28) Zayak, A. T.; Hu, Y. S.; Choo, H.; Bokor, J.; Cabrini, S.; Schuck, P. J.; Neaton, J. B. Chemical Raman Enhancement of Organic Adsorbates on Metal Surfaces. *Phys. Rev. Lett.* **2011**, *106*, 083003.
(29) Wu, D.-Y.; Liu, X.-M.; Huang, Y.-F.; Ren, B.; Xu, X.; Tian, Z.-Q. Surface Catalytic Coupling Reaction of p-Mercaptoaniline Linking to Silver Nanostructures Responsible for Abnormal Sers Enhancement: A DFT Study. *J. Phys. Chem. C* **2009**, *113*, 18212−18222.
(30) Dong, B.; Fang, Y.; Xia, L.; Xu, H.; Sun, M. Is 4-Nitrobenzenethiol Converted to P,P'-Dimercaptoazobenzene or 4-Aminothiophenol by Surface Photochemistry Reaction? *J. Raman Spectrosc.* **2011**, *42*, 1205−1206.
(31) Le Ru, E. C.; Blackie, E.; Meyer, M.; Etchegoin, P. G. Surface Enhanced Raman Scattering Enhancement Factors: A Comprehensive Study. *J. Phys. Chem. C* **2007**, *111*, 13794−13803.
(32) Saikin, S. K.; Olivares-Amaya, R.; Rappoport, D.; Stopa, M.; Aspuru-Guzik, A. On the Chemical Bonding Effects in the Raman Response: Benzenethiol Adsorbed on Silver Clusters. *Phys. Chem. Chem. Phys.* **2009**, *11*, 9401−9411.
(33) Wu, D.-Y.; Liu, X.-M.; Duan, S.; Xu, X.; Ren, B.; Lin, S.-H.; Tian, Z.-Q. Chemical Enhancement Effects in Sers Spectra: A Quantum Chemical Study of Pyridine Interacting with Copper, Silver, Gold and Platinum Metals. *J. Phys. Chem. C* **2008**, *112*, 4195−4204.
(34) Baerends, E. J.; Autschbach, J. A.; Berces, A.; et al. *ADF2010*; Scientific Computing & Modeling: Amsterdam, The Netherlands, 2010.